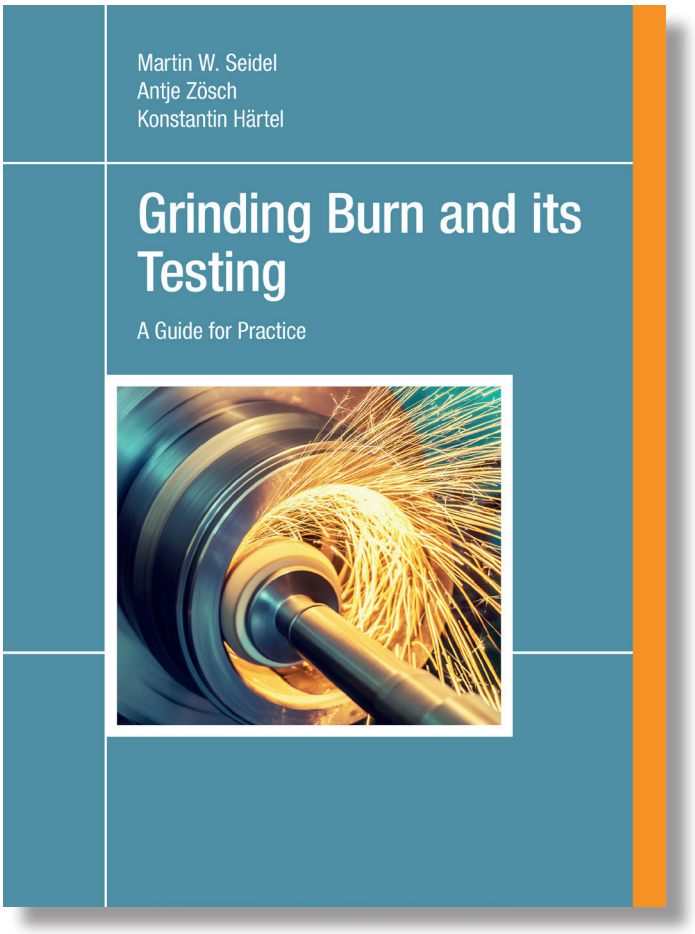

Extract from “Grinding Burn and its Testing“

by Martin W. Seidel, Antje Zösch and Konstantin Härtel

Print-ISBN: 978-3-00-070194-8
E-Book-ISBN: 978-3-00-070195-5

Further information and book orders at https://www.imq-gmbh.com/en/services/grinding-burn-detection/

Content

4 Test methods - fundamentals, possibilities and limits

4.1 Overview

Various test methods can be considered for the grinding burn detection. Depending on the method, different properties of the tempered or re-hardening zones are used to detect them. In table 4.1, the different test methods are assigned to the characteristics of tempered and re-hardening zones.

Table 4.1 Assignment of the test methods to the characteristics of the tempered and re-hardening zones

Property	Tempered zone	Re-hardening zone	Testing methods
hardness	low	high	microhardness testing
persistency to acids	low	high	nital etching (surface temper etch inspection) metallography
residual stress	tensile stress	compressive or tensile stress	X-ray microstructure analysis
electromagnetic properties	magnetically "softer"	magnetically "harder"	Barkhausen noise method Eddy current testing micromagnetic 3MA method
surface cracks			eddy current testing magnetic particle testing dye penetrant testing ultrasonic testing
hidden cracks			(magnetic particle testing) ultrasonic testing

The hardness differences between tempered and re-hardening zones on the one hand and their undamaged environment on the other hand are exploited in small load and microhardness testing. Metallographic methods are based on the different resistance of martensite and retained austenite to acids and other strong oxidizing agents. X-ray microstructure analyses are based on the fact that residual stresses lead to changes in the distance of the lattice planes in the crystal. The above-mentioned tests are usually not performed directly on the component but on machined samples and are generally time-consuming. This means that a longer time elapses between the extraction of the sample and the availability of the test result. In addition, due to the destruction of the manufactured components, testing can only be carried out on a random basis. Following a suggestion in /KAR1995/, the above-mentioned test methods are assigned to the group of laboratory methods. These are dealt with in Section 4.2.

Industrial methods (Section 4.3) are test methods which, due to short test times, enable larger numbers of manufactured components to be tested in a short time without destroying them. These include the Nital etching method (also called surface temper etch inspection), eddy current testing, the Barkhausen noise method and the micromagnetic 3MA method as well as methods for surface crack detection.

Nital etching (Section 4.3.1) as well as metallography, is based on the resistance to acids, in particular to nitric acid. If the nital etching is carried out according to the standard, the acid usually causes only a very slight removal of the surface /ZÖ2017/. However, the discoloration of the component surface can be disturbing. Therefore, this test is sometimes referred to as quasi-nondestructive.

Eddy current testing, the Barkhausen noise method and the micromagnetic 3MA method belong to the group of electromagnetic testing methods (Section 4.3.2) and are based on the different electrical and magnetic properties of tempered and re-hardening zones. These test methods act non-destructively directly on the component and can often be performed within manufacturing cycle times. However, they always require calibration on components with known properties, i.e. in the case of grinding burn testing, on components with defined tempered or re-hardening zones.

Surface cracks that are present in the component after grinding can be detected by dye penetrant inspection, magnetic particle inspection and ultrasonic inspection. Hidden cracks can be indicated by ultrasonic testing and, if they start just below the surface, by magnetic particle testing under certain conditions.

For the interpretation of the test results, it is necessary that the principle of the method is understood and, in particular, that the application limits are known. Otherwise, there is a risk of misinterpretation of the test results.

Therefore, in addition to the principle of the method, the application limits and sources of possible misinterpretations will be discussed in particular in the following chapters.

Using the before mentioned test methods, the components are examined in separate test facilities after completion of the grinding process. The manufacturing process then generally continues, so that further components with grinding burns may be manufactured until the test result is available. Hence, there is a need for so-called online monitoring systems that can register the development of the grinding burn during grinding by means of suitable sensor technology. For this purpose, /SAX1997/ investigated the physical principles of signal generation and signal propagation for the detection of grinding burn by acoustic emission analysis. Using the example of external cylindrical grinding and gear grinding, it was shown that it is possible to distinguish thermally damaged components from good parts by means of evaluation algorithms created with artificial neural networks. However, the widespread introduction of acoustic emission analysis for monitoring entire production lines is inhibited by the high cost of the equipment. This is necessary to separate the grinding burn signals from the interference signals of the grinding machine and the process.

4.2 Laboratory methods

4.2.1 Metallography and hardness testing

Metallography

A metallographic examination begins with the production of a microsection. In this process, a segment is first machined out of the component using an abrasive cutting machine.

During cutting, the workpiece must not be heated in such a way that tempered areas are created and thus grinding burn is simulated.

A particular challenge when using common abrasive cut-off machines is that the cutting discs are often much wider than the tempered zone to be found. The separation of the components must therefore take place immediately adjacent to the suspected zone. After that, the separated components must be embedded and then systematically ground down to the point where the microsection is as centered as possible in the tempered or re-hardening zone. The samples must be embedded in such a way that the embedding medium encloses the sample completely and without gaps. Otherwise, during subsequent etching, etchant running

out of the gaps can cause false indications that lead to misinterpretations.

Etching with dilute nitric acid is based on the fact that tempered zones are attacked more strongly than the martensite surrounding this zone. They therefore appear dark under the microscope /ECK1969/. The re-hardening zones, in turn, consist of very fine-grained martensite and residual austenite. The extremely fine-grained martensite and the retained austenite, which is not attacked by nitric acid, are responsible for their "white coloration" / ECK1969 , TÖ1998, ANG2006/. In the literature, these re-hardening zones are therefore often referred to as white layers. Figure 4.1 shows examples of re-hardening zones with tempered zones surrounding them on the raceway of a roller bearing outer ring.

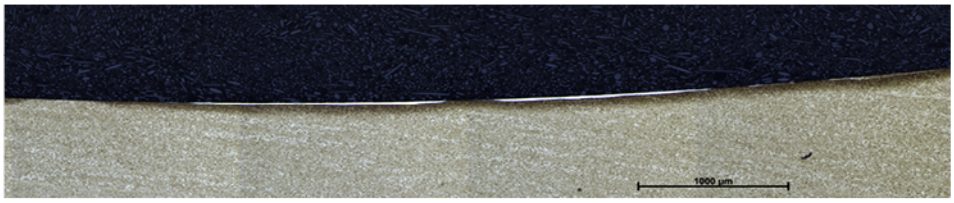

Figure 4. 1 Microsection of a roller bearing outer ring with spotted re-hardening zones and tempered zones, etched with 3% alc. HNO_3 (Source: imq)

The re-hardening zones are clearly separated from the surrounding areas. Their depth can thus be determined quite accurately in the microsection. The darker coloration of the tempered zones, on the other hand, gradually merges with the lighter coloration of the unaffected area. Here, therefore, a uniform determination of the grey value at which the transition to the basic structure has occurred is required.

Experience shows that tempered zones of small depth (10 µm can be assumed as a guide value) can only be detected with great effort.

The correct execution of all the preparation steps listed is decisive for the informative value of the microsections. A reliable metallographic examination is only possible if it is performed in a well-equipped metallographic laboratory by experienced and trained testing personnel.

Small load and micro hardness testing

Tempered and re-hardening zones can also be measured by means of small load and microhardness testing. Hardness indentations are placed on the microsection, starting near the sample edge. Figure 4.2 shows hardness indentations in a re-hardening zone and in the surrounding tempered zone. The lower part of the figure shows the measured hardness depth profile.

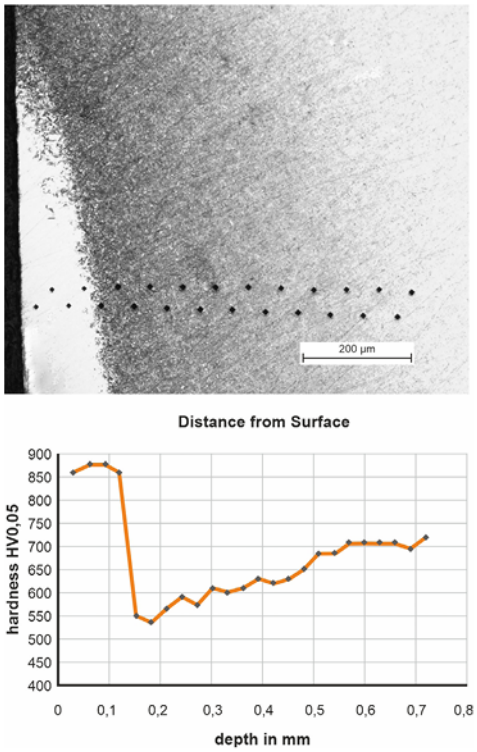

Figure 4.2 Microhardness testing of a re-hardening zone surrounded by a tempered zone, generated by laser treatment; upper Fig.: Microsection, etched with 3% alc. HNO_3, lower Fig.: Graph of hardness versus distance from the surface HV0,05 (Source: imq 2020)

The re-hardening zone exhibits hardnesses of over 850 HV0.05. From a depth of 0.1 mm, the hardness drops to values close to 500 HV0.05, and then gradually rises to the value of the undamaged zone of approximately 700 HV0.05. This is reached at about 0.5 mm.

The test is carried out in accordance with DIN EN ISO 6507 and, depending on the depth of the tempered and re-hardening zones, can be carried out with loads between 10 and 0.05 N. The distance between the hardness indentations and the sample edge and between the hardness indentations themselves must be large enough to ensure that they do not influence each other. The distance between the hardness indentations should be 2 to 3 times greater than the diagonal of the indentations. In order to nevertheless obtain a sufficiently fine depth resolution, two parallel rows of indentations were set here. An overview of the edge distances to be observed for different test loads is given in the appendix. In the above example, HV0.05 was used for testing. Assuming a hardness of 900 to 1000 HV in the re-hardening zone, the distance between the first measuring point and the edge must be greater than 0.01 mm. It can be concluded from this that the re-hardening zones in particular, which are often only a few µm thin, cannot be characterized by means of microhardness testing.

Hardness measurements on the component surface

It is also frequently asked whether grinding burn can be detected on the components by measuring the surface hardness. To answer this question, the depth of the resulting hardness indentations must be considered. In the Rockwell method with diamond cone (HRC), these have a depth of approx. 0.1 mm. In the Vickers test with a load of 100 N (HV10), the depth of indentation is approx. 0.03 to 0.05 mm. If the hardness of a tempered or re-hardening zone is to be determined approximately correctly, both its lateral extent and its depth extent must be significantly greater than the width and depth of the hardness indentations. Otherwise, one determines a "mixed" value that reflects not only the hardness of the grinding burn zone but also the hardness of underlying or adjacent undamaged areas. Re-hardening zones are often only a few µm thick. For this reason, they are penetrated by the indentation body during the test according to both HRC and HV10. The hardness values measured then primarily reflect the hardness of the underlying areas and not that of the re-hardening zone.

The hardness can also be determined by means of *mobile hardness testing* using the *ultrasonic contact impedance (UCI) method* /TIETZE2015/. Here, special hardness probes are placed on the component surface manually or with a device. As with the classic Vickers hardness, measurements can be made with different test forces from 1N to 100N. If, for example, 1N is used, hardness indentations of a depth of 0.002 to 0.003 mm are obtained. To obtain reliable measured values, the roughness of the surface must not exceed 1/3 of the indentation depth, i.e. < 0.001 mm. Fig. 4.3 shows UCI hardness curves over the surfaces of induction-hardened crankshafts into which an tempered zone has been introduced with a laser.

The tempered zone can be detected very well. However, this was only possible because the probes were not placed on the surface manually but with a device /ZÖ2016/.

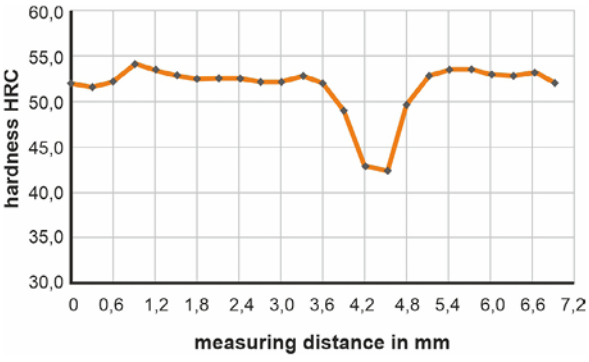

Figure 4.3

Graph of UCI-hardness F=1N across the surface of an inductively case-hardened crankshaft with a tempered zone generated by laser treatment (according to /ZÖ2016/)

In conclusion, it can be estimated that the classic hardness test is not suitable for detecting grinding burn. If the probes are guided with a fixture, tempered zones can be detected by means of the UCI method with low test forces. In general, however, surface hardness testing must take into account that the resulting hardness indentations represent damage to the surface and that these can be the starting point for cracks. In this respect, surface hardness testing does not belong to the group of non-destructive testing methods.

4.2.2 Residual stress measurements

The residual stresses in components can be measured using various methods. The X-ray diffraction method (XRD) /MACH1961, TIETZ1982, KRI1990, SPIE2019/ is frequently used to determine residual stresses in ground components.

Monochromatic X-rays are directed onto the component surface. These penetrate only a few micrometers deep into the material. The beams are diffracted at the electron shells of the atoms. The "reflected" waves emanating from the individual atoms superimpose. At certain angles of incidence, these waves amplify, and X-ray interference lines characteristic of the respective material are produced. These are registered in a detector. According to BRAGG, the angles at which the interference lines occur depend solely on the wavelength of the X-ray radiation and the distance between the lattice planes. This is shown schematically in Figure 4.4. Figure 4.5 shows an example of the diffraction pattern of pure iron.

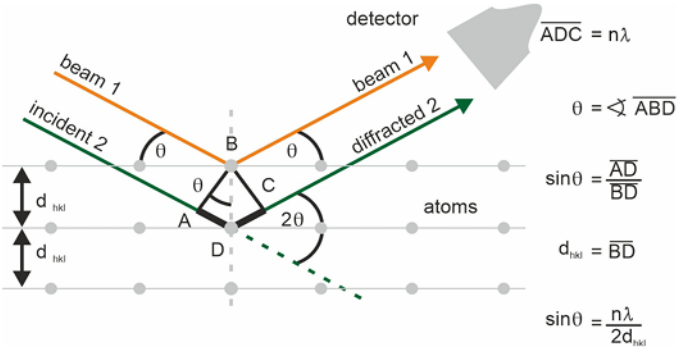

Figure 4.4 Scheme of Bragg-reflection (according to /SPIE2019/)

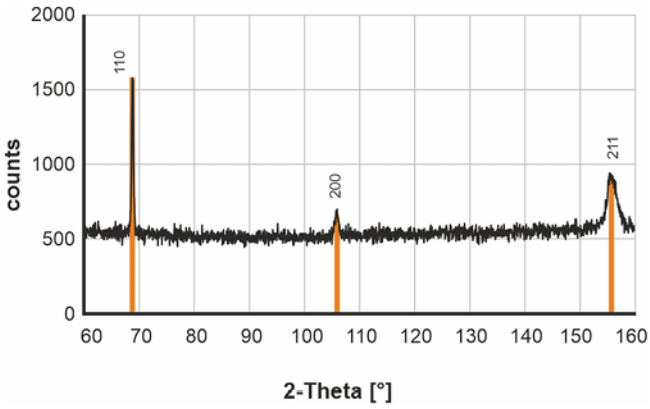

Figure 4.5 Diffraction pattern of pure iron with interference fringes of the (110), (200) and (211) lattice plane, measured by applying Cr-radiation (according to /SPIE2019/)

Residual stresses now cause a change in the spacing of the lattice planes and thus a change in the angle at which the X-ray interferences occur (Fig. 4.6). From this angular change Δθ, the macroscopic residual stresses acting in the component can be calculated.

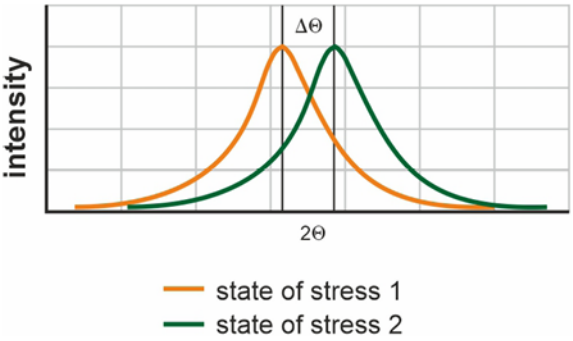

Figure 4.6 Effect of microscopic residual stress on the diffraction pattern (schematized) (Source: imq 2020)

The microscopic residual stresses caused in the material by *dislocations and foreign atoms* cause a broadening of the X-ray interference lines (Fig.4.7). Their full width at half maximum (FWHM) is therefore often used as a measure of the microstresses.

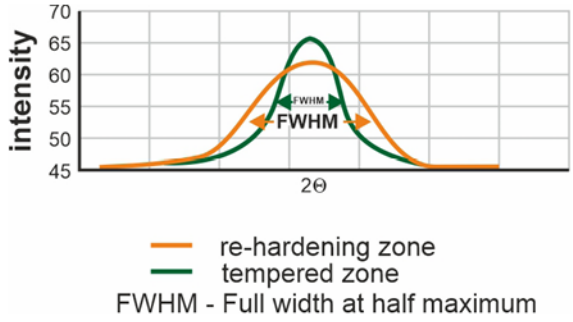

Figure 4.7 Effect of microscopic residual stress on the diffraction pattern (schematized) (Source: imq 2020)

Residual stress measurements are performed using X-ray diffractometers. These are usually stationary systems in which smaller components and separated samples can be examined. There are also mobile systems with which it is possible to determine residual stresses on larger components.

When used for residual stress measurement on components damaged by grinding burn, some special features of the method must be taken into account.

The focus of the X-ray beam determines the lateral resolution of the measurements. This is between 0.05 and 10 mm. The selected focus must therefore be adapted to the lateral extent of the grinding burn damage. It should be noted that the measurement times increase sharply as the focus becomes smaller.

Another consideration for both the selection of the method and the interpretation of the results is the penetration depth of the X-rays. This depends on the type of radiation and the angle of incidence Θ. The latter should, if possible, assume values between 70 and 80 degrees, as this provides the best conditions for determining the lattice plane spacing. In the appendix, penetration depths for Cr, Co, Cu and Mo $K_{\alpha 1}$ radiation are listed. For Cr-radiation, the reflection of the (211) lattice plane best fulfills the above condition. Here, the depth from which 63% of the information originates is about 5.5 µm. For Co-radiation, the (310) reflex should be used. The main part of the information comes there from a depth of approx. 11 µm. When measuring with Cu-radiation at the (310) reflex, the penetration depth is less than 2 µm. However, the measurement with Cu-radiation has a higher error rate, because here measurements are taken at smaller angles Θ.

Particular attention must be paid to the penetration depth for residual stress measurements on thin re-hardening zones. Often these “white layers” are only a few micrometers thick. The X-rays then also detect the tempered zones underneath. The residual stresses measured and also the retained austenite contents determined by X-ray then represent not only the re-hardening zone but also the residual stresses in the underlying tempered zone.

By means of the X-ray diffraction method, it is also possible to determine the directional dependence of the residual stresses, for example by measuring the stresses perpendicular and parallel to the grinding direction. In this case, measurements must be made in three axes. This increases the overall measurement effort.

4.3 Industrial methods

4.3.1 Nital etching

Standardization

The so-called nital etching, named after the used chemical reagents, is the only standardized method for grinding burn testing to date. In international standards and English-speaking countries for the same testing method the term Surface Temper Ech Inspection (STE) is commonly used, too.

Currently applicable standards for grinding burn testing are compiled in the appendix.

The test method described in the ISO 14 104 standard is specifically aimed at gearbox part production but can also be used for other groups of components such as roller bearing parts. The AMS 2649 standard concerns the testing of high-strength steel components for aerospace applications. In MIL-STD-867, special concerns of military aerospace such as testing of components remanufactured by grinding are considered.

AS7108/2 defines the requirements for accreditation of testing laboratories for grinding burn testing using nital etching specifically for the aerospace industry. SAE ARP 1923 describes conditions for the training of grinding burn inspectors.

Preparation and execution

The standards mentioned describe a chemical etching method for the detection of grinding burn on component surfaces. Etching is carried out either with aqueous or with alcoholic nitric acid (nital acid).

When aqueous solutions are used, higher demands must be met for cleaning the components to be tested than when alcoholic solutions are used. In addition, the etching times are much shorter than when etching in alcoholic solutions. As a result, there is a greater risk that the components will generally be etched too darkly. Grinding burn can then no longer be reliably detected, since the grinding

burn is then not distinguishable from the likewise dark surroundings.

The use of alcoholic nitric acid is somewhat easier to handle in terms of cleaning and etching times but is more problematic for reasons of environmental protection and occupational safety. For example, when testing using alcoholic acids, devices must be available to extract the evaporated alcohol. In large-scale plants for testing entire production batches (100% testing), aqueous acid is therefore primarily used.

Nital etching is a multi-stage testing process. The individual steps can be seen in the figures Figure 4.8 and Figure 4.9.

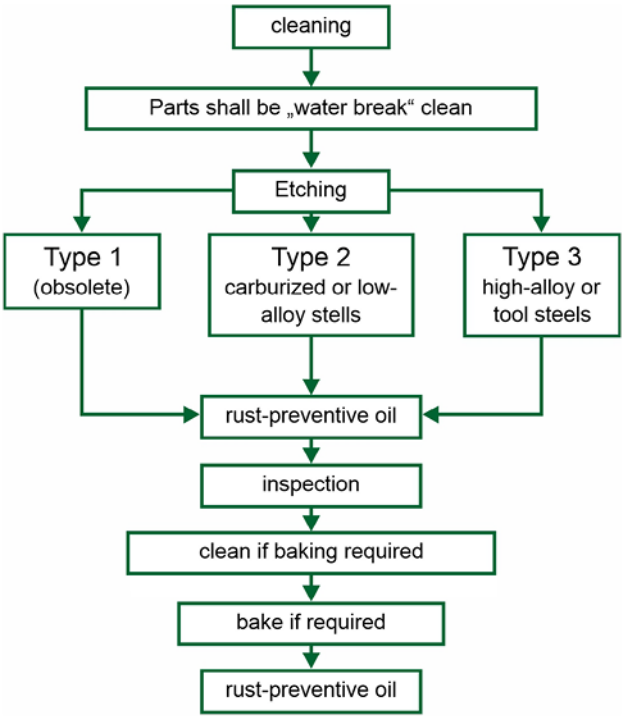

Figure 4.8 Workflow of the nital etching process according to ISO 14 104 - scheme of the entire process (Source: /ISO 14 104/)

The surfaces to be tested must be free of build-up, contamination, grease and oil. Therefore, the components must be thoroughly cleaned before etching. For verification purposes, a water-wetting test, the so-called "water break"-free test, is carried out, in which the water film on the component surface must not break for at least 15 seconds. As with metallographic preparation (Section 4.2.1), the test effect of nital etching is that tempered zones and re-hardening zones are affected differently by the acids. The method can be used for steel components made of unalloyed or low-alloyed steel. Nitrated components cannot be tested. To test components made of higher alloy steels, it is necessary to remove the passive layer that forms on such steels. This can be done by exposing the part to be tested to dilute hydrochloric acid before the actual nital etching.

Fig. 4.9 Workflow of the nital etching process according to ISO 14 104 - Etching and bleaching subprocess (Source: imq)

Step	Process	Solution
1	Nitric acid etch	Nitrit acid, 1,5% to 5% (by volume) - in alcohol or water
2	Rinse	Water or aclohol
3	Alcohol dip	Alcohol
4	Bleach	Hydrochloric acid, 2% to 6% (by volume) - in alcohol or water
5	Rinse	Water
6	Neutralize	Alkali solution pHz 10
7	Rinse	Water
8	Dry	Alcohol or hot water
9	Oil	Rust-preventive

The actual etching itself is subdivided into several subprocesses (Figure 4.9). The standards provide for etching in nitric acid and bleaching in dilute hydrochloric acid. During bleaching, the dark coating formed during etching in nitric acid is removed. This increases the contrast between the areas with grinding burn and the undamaged areas. The rinsing processes to be carried out in between are intended to prevent acids from being carried over from one bath to the next.

It is essential that the test is performed immediately after grinding and before any subsequent processes such as finishing, shot peening, etc.

As already discussed above, the tempered and re-hardening zones created during grinding can be covered by a thin solidified zone. They are then no longer visible during etching, although they are actually still present under this layer.

Index